Quantitative mass spectral evidence for the absence of circulating brain natriuretic peptide (BNP-32) in severe human heart failure

Adam M. Hawkridge[†], Denise M. Heublein[‡], H. Robert Bergen III[†], Alessandro Cataliotti[‡], John C. Burnett, Jr.[‡§], and David C. Muddiman[†§¶‖]

[†]W. M. Keck FT-ICR Mass Spectrometry Laboratory and Mayo Proteomics Research Center, [‡]Division of Cardiovascular Diseases, and [¶]Department of Biochemistry and Molecular Biology, Mayo Clinic College of Medicine, Rochester, MN 55905

Communicated by John B. Fenn, Virginia Commonwealth University, Richmond, VA, October 6, 2005 (received for review September 10, 2005)

C-terminal brain (B-type) natriuretic peptide (BNP)-32 is a widely used clinical biomarker for the diagnosis, prognosis, and treatment of heart failure (HF). The 32-aa peptide is synthesized primarily in the atrial and ventricular myocardium and constitutes the mature biologically active form of immature BNP (pro-BNP). There has been mounting evidence that suggests BNP circulates in different structural forms that impact HF diagnosis and *in vivo* activity. Herein, we have developed and used an immunoaffinity purification assay to isolate endogenous BNP-32 from New York Heart Association class IV patient plasma for subsequent analysis by nano-liquid chromatography (LC) electrospray ionization Fourier transform ion cyclotron resonance (FT-ICR) MS. We have introduced stable isotope-labeled BNP-32 to the assayed plasma to enable quantification of endogenous levels of BNP-32. Unlike the chemically nonspecific point-of-care tests (POCTs) and RIAs used worldwide to quantify BNP-32 from plasma, FT-ICR-MS (unprecedented mass measurement accuracy) coupled with LC (retention time) affords extraordinary molecular specificity, and when combined with the use of internal standards is able to confidently identify and quantify BNP-32. The significance of this work is despite exceedingly high circulating levels of BNP-32 in the New York Heart Association class IV patients as determined by POCTs (>290 fmol/ml) nano-LC-electrospray ionization-FT-ICR-MS data did not reveal any endogenous BNP-32. These results provide molecularly specific evidence for the absence of circulating BNP-32 in advanced-stage HF patients and suggest the existence of altered forms of BNP that are contributing to the POCT values.

biomarkers | electrospray ionization | Fourier transform-ion cyclotron resonance MS | immunoaffinity purification | targeted proteomics

Heart failure (HF) is a highly prevalent form of cardiovascular disease that currently afflicts >5 million Americans (1, 2). In 2004, HF was diagnosed in ≈550,000 new patients and attributed to ≈300,000 deaths. The annual direct and indirect costs associated with diagnosing, monitoring, and treating HF has been estimated to be >$25 billion in the United States. Recently, numerous advances in the diagnosis and treatment of HF have been introduced that offer more rapid, lower-cost alternatives to traditional diagnostic tools and therapies (3).

Brain (B-type) natriuretic peptide (BNP) has emerged in recent years as an effective diagnostic and prognostic cardiac biomarker for HF (4–10). Commercially available point-of-care tests (POCTs) have been developed for rapidly determining BNP levels in patients and have found widespread use in clinics, hospitals, and urgent-care facilities worldwide (10–12). These tests provide invaluable, real-time diagnostic information to health-care deliverers who can quickly diagnose patients presenting with HF symptoms (e.g., shortness of breath, chest pain) (5, 7). After diagnosis, the POCT has been used as a cost-effective means for monitoring HF treatment efficacy. Furthermore, recombinant BNP has been administered to hospitalized, advanced-stage HF patients with improvement in symptoms and cardiac-filling pressures (13, 14). However, despite the excellent specificity and sensitivity of BNP POCT along with its therapeutic potential, significant questions remain as to the exact function(s) and form(s) of circulating BNP, which, if altered, could contribute to the pathophysiology of HF.

BNP is synthesized primarily in the cardiac atria and ventricle where it acts as an antagonist to the progressive effects of HF. BNP is initially synthesized as a 134-aa peptide that is subsequently processed to form a 108-aa peptide (pro-BNP) (15, 16). The pro-BNP is enzymatically cleaved to form a 76-aa N-terminal (NT) peptide (NT-pro-BNP) and a biologically active 32-aa C-terminal peptide (BNP-32). As the pressure load in the left ventricle increases at the onset of HF, BNP-32 is upregulated to relieve congestion associated with the effects of ventricular remodeling, cardiac hypertrophy, and loss of contractibility. However, several reports have challenged the assertion that BNP circulates in only two distinct forms (i.e., NT-pro-BNP and BNP-32) (16–20). Studies using a combination of RIA and size exclusion chromatography have reported the existence of higher-molecular-mass forms of BNP in blood that range from 12 to 48 kDa. Researchers have speculated that these forms may be uncleaved pro-BNP (monomer) or noncovalently linked trimers or tetrameters of pro-BNP (17–20). However, unambiguous *in vivo* structural identification of these species remains elusive. The existence of altered forms of BNP would have a profound impact on the diagnosis and treatment of HF because these species could have reduced *in vivo* activity and potentially interfere with widely used POCTs (21, 22).

To test these hypotheses, we have implemented nano- liquid chromatography (LC) electrospray ionization (ESI) Fourier transform (FT) ion cyclotron resonance (ICR) MS to study New York Heart Association (NYHA) class-IV patients in an effort to quantify circulating BNP-32 levels with unprecedented molecular specificity. HF patients were initially diagnosed with commercially available POCTs and determined to have high levels of BNP-32 (>290 fmol/ml). After diagnosis, additional patient samples were collected for nano-LC-ESI-FT-ICR MS analysis and BNP-32 quantification. An immunoaffinity purification assay was used to target BNP-32 in these patient plasma samples, and endogenous BNP-32 levels were quantified by using isotope dilution MS. The significant finding of this research was that no endogenous BNP-32 was detected by MS in plasma from NYHA class-IV patients despite predetermined POCT levels of

Conflict of interest statement: No conflicts declared.

Abbreviations: BNP, brain (B-type) natriuretic peptide; HF, heart failure; NYHA, New York Heart Association; POCT, point-of-care test; LC, liquid chromatography; ESI, electrospray ionization; FT, Fourier transform; ICR, ion cyclotron resonance.

[§]To whom correspondence may be addressed. E-mail: burnett.john@mayo.edu or david_muddiman@ncsu.edu.

[‖]Present address: W. M. Keck FT-ICR Mass Spectrometry Laboratory, Department of Chemistry, North Carolina State University, Raleigh, NC 27695.

www.pnas.org/cgi/doi/10.1073/pnas.0508782102

BNP-32 exceeding 290 fmol/ml, which suggests that in these studies POCTs specific to BNP-32 are measuring altered forms of BNP (potentially high-molecular-weight forms), metabolically degraded BNP-32, and/or other biomolecular species that cross-react with the antibody.

Materials and Methods

Materials. Stable isotope-labeled BNP-32 (BNP-32*) was synthesized in the Mayo Proteomics Research Center with an Applied Biosystems 433A peptide synthesizer by using recommended procedures for HBTU (*O*-(benzotriazole-1-yl)-1,1,3,3-tetramethyluronium hexafluorophosphate) activation and coupling. The starting resin was a preloaded histidine (trityl) Wang resin. Five $^{13}C_2$,^{15}N-fluorenylmethoxycarbonyl-glycines from Cambridge Isotope Laboratories (Andover, MA) were incorporated into the BNP-32 sequence at positions 7, 9, 12, 23, and 25 to give a final mass shift of 15 Da relative to unlabeled BNP-32. The peptide was purified by RP-HPLC on a Phenomenex (Torrance, CA) 250 × 21.2 mm, 15-μm Jupiter C-18 column. Disulfide bond formation was achieved by air oxidation in ammonium bicarbonate (pH 8.5) overnight at room temperature. The amino acid composition and purity of the peptide was confirmed by dual ESI-FT-ICR MS (23) with a mass measurement accuracy of <1 ppm.

All reagents were >98% purity, and all solvents were HPLC grade (>99%). Human BNP-32 (unlabeled) was obtained from Sigma (>99%), protein A-purified rabbit anti-BNP-32 (human) IgG was obtained from Phoenix Pharmaceuticals (Belmont, CA), and suspended goat anti-rabbit IgG-modified magnetic beads (MagnaBind) were obtained from Pierce.

Patient Sample Collection and POCTs. This study was approved by the Mayo Clinic Institutional Review Board. Plasma samples were obtained from four patients, all with severe NYHA class-IV symptoms. The Triage BNP-32 POCT (Biosite, San Diego) was used to determine BNP-32 levels by using the standard protocols provided by the manufacturer.

Immunoaffinity Purification of BNP. Plasma samples were removed from the freezer (−86°C) and defrosted over ice until the matrix became slushy. The samples were then removed from the ice and allowed to sit for ≈5 min at ambient temperature to fully thaw. Five hundred femtomoles of stable isotope-labeled BNP-32* in 0.01 M PBS (pH 7.4) were added to 1-ml aliquots of NYHA class-IV plasma and vortexed thoroughly for ≈30 s. The 1-ml samples were then passed through a solid-phase extraction column (Varian, LRC BondElut C_8) and lyopholized. Rabbit anti-BNP-32 (human) primary antibody (7.5 μg) was added to the reconstituted extract (1 ml of 0.01 M PBS, pH 7.4) and incubated for 1 h at 8°C. Seventy five microliters of the goat anti-rabbit secondary antibody suspension was added and vortexed at ambient temperature for 1 h. The antibody–antigen complexes were separated, washed with 1 ml of 0.01 M PBS (pH 7.4), released (450 μl, 90:10, H_2O/ACN with 1.0% trifluoroacetic acid and 0.001% Zwittergent 3–16), filtered (Microcon 100-kDa cut-off filter, Millipore), and lyophilized. Samples were reconstituted for mass spectral analysis in 50 μl of 0.001% Zwittergent 3–16 (Calbiochem).

Instrumentation. Nano-LC-ESI-FT-ICR MS experiments were carried out on an Eksigent (Livermore, CA) direct flow, nano-LC system coupled to either an Ionspec (Lake Forest, CA) 9.4-Tesla FT-ICR mass spectrometer or a Thermo Electron (San Jose, CA) 7-Tesla linear ion trap FT-ICR mass spectrometer with a Micromass (Manchester, U.K.) nano-ESI Z-spray source or Ionmax (San Jose, CA) nano-ESI source, respectively.

Fifty-microliter samples were injected onto a custom-packed 0.25-μl C_8 (5 μm MAGIC, Michrom Bioresources, Auburn, CA) precolumn (Optimize Technologies, Oregon City, OR) and desalted followed by a 50-min binary gradient onto a 10-cm, self-packed, 75-μm i.d. Integrafrit (New Objective, Woburn, MA) C_{18} column (5 μm TARGA, Higgins Analytical, Mountain View, CA).

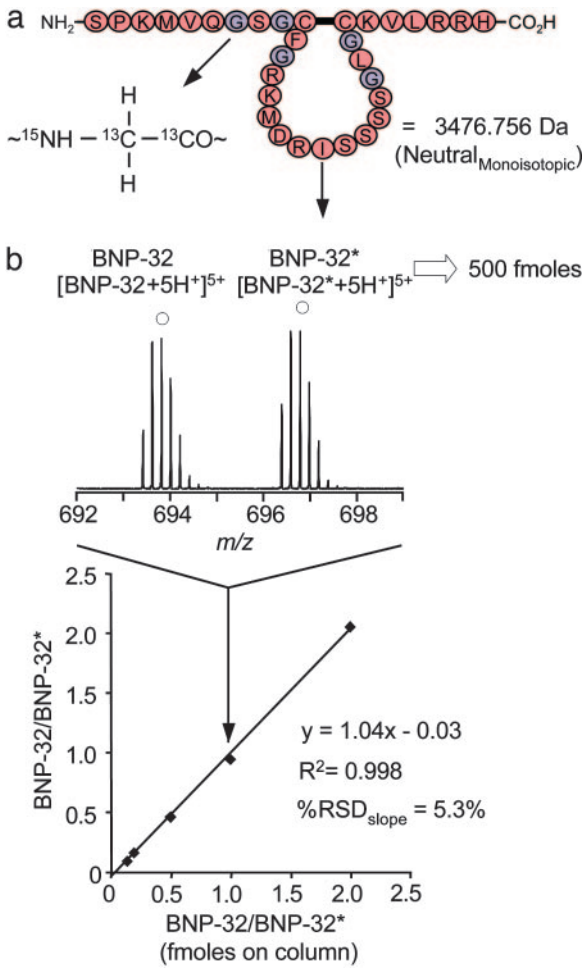

Fig. 1. Experimental approach for determining the standard curve for BNP-32. (*a*) Chemical structure of stable isotope-labeled BNP-32 (BNP-32*). (*b*) Standard curve for BNP-32 using data derived from nano-LC-ESI-FT-ICR MS data. A representative FT-ICR mass spectrum of the 5+ charge state from a 1:1 mixture (500 fmol each) of exogenous BNP-32 and BNP-32* is shown as an example. The ion abundances used for determining the standard curve were defined by using the A + 2 isotope from both species (denoted by ○). RSD, relative standard deviation.

Results and Discussion

The currently used assays for quantifying endogenous BNP-32 in plasma typically involve the use of N- or C-terminal BNP antibodies with some form of reporter molecule (e.g., ^{125}I radiolabel, fluorescence, and electrochemiluminescence). Although these approaches are very sensitive, they lack molecular specificity. If one assumes the existence of multiple forms of BNP that are recognized by these antibodies, then the quantitative measurement is a composite of several species and not just one specific antigen (see below). LC coupled to MS is a powerful bioanalytical technique that combines sensitivity and molecular specificity for identifying and quantifying biomolecules; the latter is accomplished by implementing internal standards (24, 25). By combining the specificity of dual-antibody purification, the retention time in nano-LC, addition of an internal standard, the precise and accurate mass measurements afforded by FT-

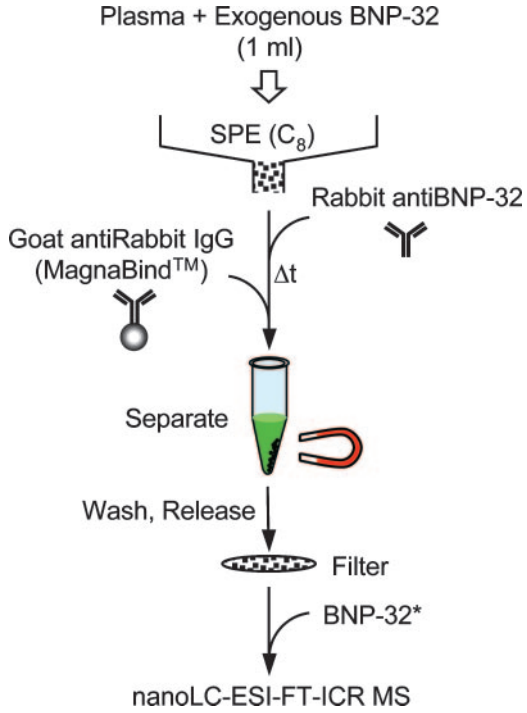

Fig. 2. Experimental approach for developing and optimizing the dual-antibody immunoaffinity purification assay for nano-LC-ESI-FT-ICR MS analysis. The general protocol was as follows: (*i*) 500 fmol of exogenous BNP-32 was added to 1 ml of healthy patient plasma (<5 fmol/ml endogenous BNP-32) and passed through a C_8 solid-phase extraction (SPE) cartridge; (*ii*) plasma is eluted and then treated with the primary antibody (rabbit anti-BNP-32); (*iii*) after a period, the secondary antibody is added (goat anti-rabbit IgG) and incubated; (*iv*) the magnetic beads with the antigen-primary-secondary complex are separated, washed, and then released; (*v*) the dissociated complex is filtered and spiked with 100 fmol of BNP-32*; and (*vii*) the resulting sample is reconstituted and analyzed by nano-LC-ESI-FT-ICR MS.

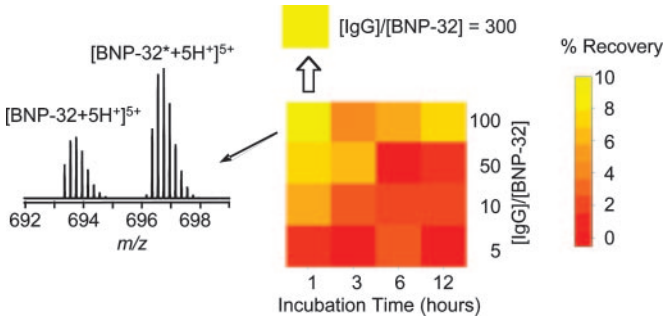

Fig. 3. Heat map showing the percentage of BNP-32 recovery from plasma as a function of incubation time and primary antibody concentration. The FT-ICR mass spectrum of recovered exogenous BNP-32 ($[BNP\text{-}32 + 5H^+]^{5+}$) and the BNP-32* ($[BNP\text{-}32^* + 5H^+]^{5+}$) internal standard under the optimal recovery conditions is shown to the left of the heat map.

ICR MS, and the potential for top-down tandem MS analysis by FT-ICR MS, it is possible to confidently identify and quantify BNP-32 and to identify novel molecular forms of BNP that cross-react with the primary antibody. FT-ICR MS represents the preeminent MS platform with unparalleled mass measurement accuracy, resolving power, and dynamic range (26, 27). Furthermore, this instrument platform has the downstream potential for identifying large intact biomolecules such as high-molecular-weight forms of BNP (e.g., tandem MS) (28).

Fig. 1*a* shows the structure of the BNP-32 internal standard with stable isotope-labeled glycines inserted into the backbone. The stable isotope-labeled BNP-32 (BNP-32*) gives a mass shift of 15 Da relative to unlabeled BNP-32 that can be readily resolved in the mass spectrum. Because BNP-32 and its isotopomer BNP-32* are chemically very similar, they have the same nano-LC retention time. The standard curve for BNP-32 measured by nano-LC-ESI-FT-ICR MS is shown in Fig. 1*b*. The ratio of BNP-32/BNP-32* MS ion abundance (A + 2 isotope) plotted versus the ratio of BNP-32/BNP-32* injected on column (fmol in 0.01 M PBS) gave a slope of 1.04 with a percent relative SD of 5.3%. During the course of these experiments, the limit of detection was determined to be ≈15 fmol of BNP-32 on column; however, in some instances we could readily detect 5 fmol of BNP-32 on column.

A representative ESI-FT-ICR mass spectrum of the 5+ charge state of BNP-32 and BNP-32* (1:1) is shown in Fig. 1*b*. The 4+, 5+, and 6+ charge states were observed; however, the 5+ charge state comprised >80% of the total ion abundance. When the amount of BNP on column approached the limit of detection, only the 5+ charge state was observed; thus, we used only the abundance of the 5+ charge state for quantification. The combination of unparalleled mass accuracy (≈1–2 ppm for FT-ICR MS) and identical LC retention times of BNP-32 and BNP-32* provides two orthogonal dimensions of data, allowing for confident identification and quantification of endogenous levels of BNP-32.

The complexity of plasma represents a formidable challenge for measuring low-level proteins and peptides by LC-MS (29). Circulating levels of BNP-32 typically range between ≈0.3 and ≈145 fmol/ml depending on the condition of the patient and severity of HF. Despite the potentially high levels of BNP-32 in advanced-stage HF, it is still ≈8 orders of magnitude lower than the most abundant species in plasma (i.e., albumin: ≈0.45–0.83 μmol/ml) (29). Therefore, to quantify BNP-32 from human plasma by nano-LC-ESI-FT-ICR MS, it was necessary to develop an immunoaffinity purification assay to target BNP-32 as well as other forms of BNP that are recognized by the primary antibody.

A dual-antibody approach was found to be the most effective at isolating BNP-32 from plasma (Fig. 2). Briefly, a primary antibody (rabbit anti-BNP-32 human) was added to solid-phase extraction (SPE) plasma to capture BNP-32 and a secondary antibody (surface-bound goat anti-rabbit) was added to isolate and purify the antibody–antigen complex. The assay in Fig. 2 was optimized by spiking 20 ml of plasma from a healthy human patient (<5 fmol of BNP-32/ml) with 500 fmol/ml of exogenous BNP-32 before assaying. After thoroughly mixing the spiked 20-ml plasma sample, the sample was split into 20 × 1-ml fractions and each passed through a separate SPE cartridge. The incubation time of the primary antibody and the primary antibody concentration were varied during the assay to determine the optimal conditions. After the assay, each sample was reconstituted in 50 μl of 0.002 μM BNP-32* in 0.001% Zwittergent 3–16 (100 fmol BNP-32* total) immediately before nano-LC-ESI-FT-ICR MS analysis as a means of quantifying the recovered BNP-32.

Fig. 3 shows a heat map representing the percentage recovery of BNP-32 from plasma as a function of incubation time and primary antibody concentration. The data showed that the recovery improved as the incubation time was reduced and the primary antibody concentration was increased. A primary antibody concentration [IgG] of 100-fold relative to the [BNP-32] incubated for 1 h was found to be optimal with no further improvement in recovery observed for higher primary antibody concentrations (e.g., [IgG]/[BNP-32] = 300).

A representative mass spectrum of recovered exogenous BNP-32 (500 fmol/ml) with 100 fmol of BNP-32* at optimal assay conditions is shown in Fig. 3 *Inset*. The highest percentage recovery for this set of samples was found to be ≈10%. Given a BNP-32 limit of detection for the nano-LC-ESI-FT-ICR MS system of ≈15 fmol, we were limited to analyzing patient plasma with a minimum of 150

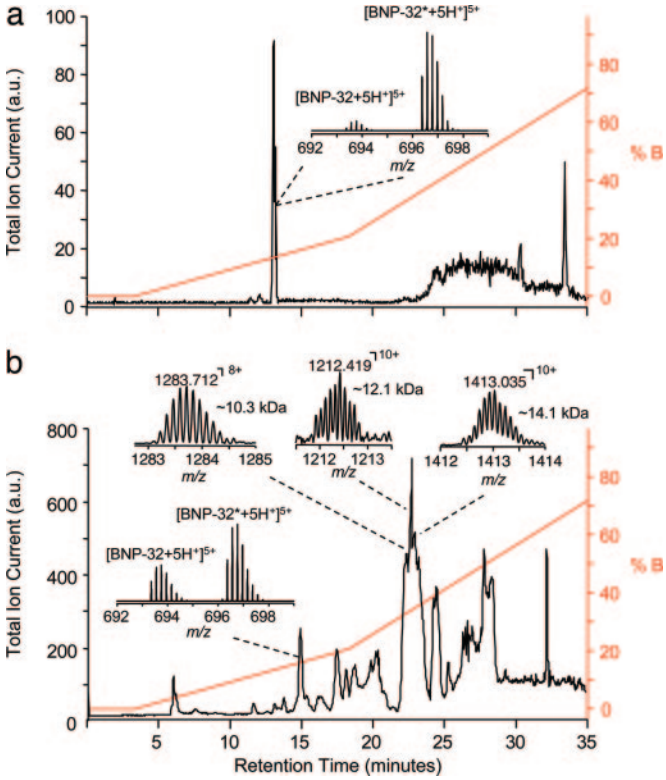

Fig. 4. Nano-LC-ESI-FT-ICR MS total ion chromatograms of 50 fmol BNP-32/500 fmol BNP-32* in PBS, pH 7.4 (*a*) and 500 fmol of exogenous BNP-32 immunoaffinity-purified from plasma obtained from a healthy individual (*b*). The left *y* axis is the total ion current in arbitrary units (a.u.), and the right *y* axis is the percentage of B mobile phase (%B) over the course of the nano-LC gradient. FT-ICR mass spectra shown in *b* are representative of the high-molecular-weight species present in the immunoaffinity-purified sample. Mass-to-charge (m/z) values for the most abundant isotope and the approximate neutral masses are shown for each isotopic distribution. The total gradient time was 50 min (shown is 0–35 min containing the relevant elution window).

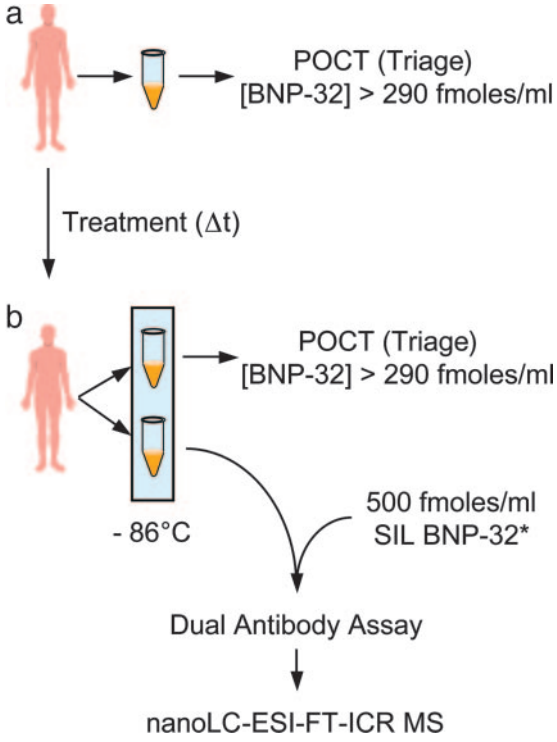

Fig. 5. Sample collection, storage, and analysis protocol for NYHA class-IV patients (Table 1). (*a*) Patients present at the Mayo Clinic with HF and are identified by POCT to have exceedingly high levels of BNP-32 (>290 fmol/ml). (*b*) Patients return for follow-up visit, and multiple blood samples are drawn, processed into plasma, and frozen at −86°C. A 1-ml plasma sample is thawed, spiked with 500 fmol of the BNP-32* standard, processed by using the dual-antibody immunoaffinity purification assay for BNP-32, and analyzed by nano-LC-ESI-FT-ICR MS. BNP-32 is measured by POCT in the second frozen sample after nano-LC-ESI-FT-ICR MS analysis to account for degradation.

fmol/ml of endogenous BNP-32, thus, our rationale for choosing patients with very high levels of BNP-32. Furthermore, experiments designed to determine the reproducibility of the assay showed a significant decrease in BNP-32 and BNP-32* absolute ion abundance after five replicate injections with blanks interdigitated (data not shown). This decrease was attributed to the filtering step in the assay that allowed high abundant proteins (e.g., antibody) into the final sample, which compromised the chromatographic column efficiency over time.

Fig. 4 shows the total ion current as a function of nano-LC retention time for BNP-32/BNP-32* spiked into PBS and immunoaffinity-purified exogenous BNP-32 from plasma with the BNP-32* internal standard, respectively. The right axes shows the nano-LC gradient profile for the B mobile phase (%B). The Fig. 4 *Insets* show the ESI-FT-ICR mass spectra of BNP-32 and BNP-32*. In addition to BNP-32 and BNP-32*, we typically observe on the order of 25–50 unique molecular species upon analysis of immunoaffinity-purified plasma from healthy individuals (Fig. 4*b*) with molecular masses ranging from 1 to >14 kDa. Representative ESI-FT-ICR mass spectra of three different species with molecular masses of 10.3, 12.1, and 14.1 kDa are shown in Fig. 4*b*. We observed these and several other large-molecular-mass species in the immunoaffinity-purified plasma, which, based solely on their masses, could be misassigned as novel molecular forms of BNP. This example, where the patient is healthy and BNP levels were predetermined by POCT to be low (<5 fmol/ml), illustrates the shortcomings associated with using only intact masses for identifying novel biomolecular species within complex samples (e.g., plasma). Thus, confident elucidation of novel molecular forms of BNP by MS demands both accurate mass data (<1–2 ppm) and top-down tandem MS of these intact forms (i.e., the generation of sequence tags). Subsequent tryptic digests of immunoaffinity-purified plasma samples, LC-tandem MS analysis of the digest, and database searching showed a large number of human serum albumin peptides (data not shown). Therefore, the high-molecular-mass species observed in Fig. 4*b* are attributed to a high abundance of plasma proteins and not BNP.

Patient records at the Mayo Clinic were monitored to identify NYHA class-IV patients with very high levels of BNP-32 (>290 fmol/ml) as determined by POCT (Fig. 5*a*). After these patients

Table 1. Data for NYHA class IV patients used in this study with BNP-32 concentrations (fmol/ml) determined by the Triage POCT

		Initial patient visit		Posttreatment visit	
Patient	Sex	Date	[BNP-32], fmol/ml	Date	[BNP-32], fmol/ml
1	Female	3/25/05	627	4/18/05	393
2	Female	3/14/05	653	4/18/05	340
3	Male	3/17/05	420	4/20/05	251
4	Male	3/15/05	<1,156	NA	NA

The dates correspond to the POCT measurement. NA, a follow-up sample from patient 4 was not available.

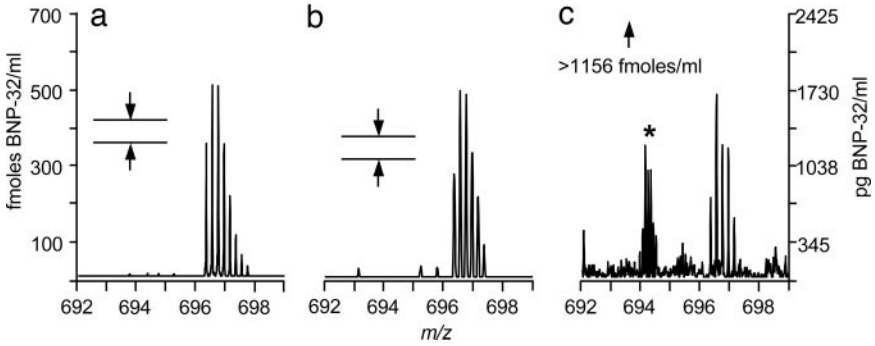

Fig. 6. Absolute quantitative nano-LC-ESI-FT-ICR mass spectral results from immunoaffinity-purified NYHA class-IV patient samples with 500 fmol of BNP-32* internal standard. The left *y* axis is fmol of BNP-32/ml of plasma, and the right *y* axis is pg of BNP-32/ml of plasma. All three spectra show significant ion abundances for the BNP-32* standard ([BNP-32* + $5H^+$]$^{5+}$) (500 fmol/ml) but no endogenous BNP-32 was detected by nano-LC-ESI-FT-ICR MS in any of the samples. The arrows represent the expected ion abundances for endogenous BNP-32 based on the POCT. Spectra are for patient 1 (*a*), patient 2 (*b*), and patient 4 (*c*). * in *c* denotes the isotopic distribution for a high-molecular-weight species that coeluted with BNP-32*.

presented with NYHA class-IV HF, they were subsequently treated over a period and then recalled for follow-up visits at the clinic. During the follow-up visits, multiple plasma samples were collected and frozen (−86°C) until they were assayed for POCT and MS analysis (Fig. 5*b*). The MS data were collected on 4/14/05 and 4/15/05, which was before the POCT measurements so as to account for any potential BNP-32 degradation. Four NYHA class-IV patient samples were obtained that met these criteria and are shown in Table 1. All four patients, with the exception of patient 4 (second sample was not available), were found by POCT to have BNP-32 levels >290 fmol/ml immediately after nano-LC-ESI-FT-ICR MS analysis; dates shown are for POCT measurements. To quantify endogenous BNP-32 in each of these samples by MS, 500 fmol of BNP-32* was added to each 1 ml of NYHA class-IV plasma sample before processing with the dual-antibody assay (Fig. 5*b*). By spiking in the internal standard before applying the assay, the error associated with recovery of endogenous BNP-32 is eliminated.

Fig. 6 shows representative ESI-FT-ICR mass spectra from three of the NYHA class-IV patients listed in Table 1. The most striking result from these three spectra was the absence of endogenous BNP-32. The BNP-32* internal standard was observed in all of the spectra with very strong ion abundances in Fig. 6 *a* and *b* and modest ion abundance in Fig. 6*c*. The inset arrows in each mass spectrum indicate where the endogenous BNP-32 signal should be based on the POCT levels. Given that the ion abundances are very high for the mass spectra in Fig. 6 *a* and *b*, the lack of any endogenous BNP-32 signal convincingly suggests that the POCT for these two samples is incorrect with respect to BNP-32 levels. The weaker ion abundance for BNP-32* in Fig. 6*c* suggests that the assay did not recover as much as is typically observed (data not shown) and that the trapping efficiency of the precolumn has declined. However, the endogenous BNP-32 level should be twice as much based on the POCT value. The species denoted by * in Fig. 6*c* is an 8-kDa species (12+ charge state) that coeluted with BNP-32 but does not appear to be related to BNP. The mass spectral results for patient 3 did not show either endogenous BNP-32 or BNP-32* (data not shown). However, significant ion abundances were observed for oxidized BNP-32* (methionine oxidation), which is commonly attributed to sample handling. A comprehensive search of all mass spectra in each sample chromatogram did not show evidence for oxidized endogenous BNP-32 (methionine oxidation) or degradation products of BNP-32 that have previously been reported (e.g., BNP-3-32) (30, 31).

Since the initial discovery of BNP-32 by Sudoh *et al.* (32) >15 years ago, investigations have intensely focused on elucidating its *in vivo* function and structure and more recently its diagnostic, prognostic, and therapeutic utility. There has been growing evidence that the roles and forms of BNP are not as well understood as previously thought. However, a lack of chemically and structurally specific evidence for these findings has hindered the advancement of these theories. We have shown here conclusive evidence that a widely used POCT for measuring BNP-32 is identifying forms of BNP different from the biologically active BNP-32. Although our findings do not call into question the diagnostic and prognostic utility of the POCT, they do provide strong evidence that cross-reactive species (BNP-related or unknown) are contributing to the POCT measurement.

Future studies should identify the circulating forms of BNP that are being measured by POCT, which would certainly be a breakthrough, and subsequently evaluate them for diagnostic, prognostic, and therapeutic value. Moreover, it is essential that we determine whether these results are reproducible across gender, age, and race given that these data do not represent a cross section of the broader population. These additional measurements should be facilitated by continuing to understand and optimize the sample procurement and overall analytical technology.

We thank Mr. Ben Madden for assistance with some of the measurements and Professor Steffen Heber for assistance with figures. This work was supported by the W. M. Keck Foundation (D.C.M.), National Institutes of Health Grant HL36634 (to J.C.B.), American Heart Association Grant 0365411Z (to A.C.), and the Mayo Clinic College of Medicine.

1. American Heart Association (2004) *Heart Disease and Stroke Statistics: 2004 Update* (American Heart Association, Dallas), pp. 23–24.
2. Jessup, M. & Brozena, S. (2003) *N. Engl. J. Med.* **348,** 2007–2018.
3. Hunt, S. A., Baker, D. W., Chin, M. H., Cinquergrani, M. P., Feldman, A. M., Francis, G. S., Ganiats, T. G., Goldstein, S., Gregoratos, G., Jessup, M. L., *et al.* (2001) *J. Am. Coll. Cardiol.* **38,** 2102–2113.
4. Davidson, N. C., Naas, A. A., Hanson, J. K., Kennedy, N. S., Coutie, W. J. & Struthers, A. D. (1996) *Am. J. Cardiol.* **77,** 828–831.
5. Dao, Q., Krishnaswamy, P., Kazanegra, R., Harrison, A., Amirnovin, R., Lenert, L., Clopton, P., Alberto, J., Hlavin, P. & Maisel, A. S. (2001) *J. Am. Coll. Cardiol.* **37,** 379–385.
6. Luchner, A., Burnett, J. C., Jr., Jougasaki, M., Hense, H. W., Heid, I. M., Muders, F., Riegger, G. A. & Schunkert, H. (2000) *J. Hypertens.* **18,** 1121–1128.
7. Maisel, A. S., Krishnaswamy, P., Nowak, R. M., McCord, J., Hollander, J. E., Duc, P., Omland, T., Storrow, A. B., Abraham, W. T., Wu, A. H., *et al.* (2002) *N. Engl. J. Med.* **347,** 161–167.
8. Yamamoto, K., Burnett, J. C., Jr., Jougasaki, M., Nishimura, R. A., Bailey, K. R., Saito, Y., Nakao, K. & Redfield, M. M. (1996) *Hypertension* **28,** 988–994.
9. de Lemos, J. A., Morrow, D. A., Bentley, J. H., Omland, T., Sabatine, M. S., McCabe, C. H., Hall, C., Cannon, C. P. & Braunwald, E. (2001) *N. Engl. J. Med.* **345,** 1014–1021.
10. Maisel, A. S. (2003) *Heart Fail. Rev.* **8,** 327–334.

11. Fischer, Y., Filzmaier, K., Stiegler, H., Graf, J., Fuhs, S., Franke, A., Janssens, U. & Gressner, A. M. (2001) *Clin. Chem.* **47,** 591–594.
12. Wu, A. H., Packer, M., Smith, A., Bijou, R., Fink, D., Mair, J., Wallentin, L., Johnston, N., Feldcamp, C. S., Haverstick, D. M., *et al.* (2004) *Clin. Chem.* **50,** 867–873.
13. Yoshimura, M., Yasue, H., Morita, E., Sakaino, N., Jougasaki, M., Kurose, M., Mukoyama, M., Saito, Y., Nakao, K. & Imura, H. (1991) *Circulation* **84,** 1581–1588.
14. Colucci, W. S., Elkayam, U., Horton, D. P., Abraham, W. T., Bourge, R. C., Johnson, A. D., Wagoner, L. E., Givertz, M. M., Liang, C. S., Neibaur, M., *et al.* (2000) *N. Engl. J. Med.* **343,** 246–253.
15. Baxter, G. F. (2004) *Basic Res. Cardiol.* **99,** 71–75.
16. Goetze, J. P. (2004) *Clin. Chem.* **50,** 1503–1510.
17. Yandle, T. G., Richards, A. M., Gilbert, A., Fisher, S., Holmes, S. & Espiner, E. A. (1993) *J. Clin. Endocrinol. Metab.* **76,** 832–838.
18. Seidler, T., Pemberton, C., Yandle, T., Espiner, E., Nicholls, G. & Richards, M. (1999) *Biochem. Biophys. Res. Commun.* **255,** 495–501.
19. Shimizu, H., Masuta, K., Aono, K., Asada, H., Sasakura, K., Tamaki, M., Sugita, K. & Yamada, K. (2002) *Clin. Chim. Acta* **316,** 129–135.
20. Tateyama, H., Hino, J., Minamino, N., Kangawa, K., Minamino, T., Sakai, K., Ogihara, T. & Matsuo, H. (1992) *Biochem. Biophys. Res. Commun.* **185,** 760–767.
21. Apple, F. S., Panteghini, M., Ravkilde, J., Mair, J., Wu, A. H., Tate, J., Pagani, F., Christenson, R. H. & Jaffe, A. S. (2005) *Clin. Chem.* **51,** 486–493.
22. Ala-Kopsala, M., Magga, J., Peuhkurinen, K., Leipala, J., Ruskoaho, H., Leppaluoto, J. & Vuolteenaho, O. (2004) *Clin. Chem.* **50,** 1576–1588.
23. Nepomuceno, A. I., Muddiman, D. C., Bergen, H. R., Craighead, J. R., Burke, M. J., Caskey, P. E. & Allan, J. A. (2003) *Anal. Chem.* **75,** 3411–3418.
24. Aebersold, R. & Mann, M. (2003) *Nature* **422,** 198–207.
25. Aebersold, R. & Goodlett, D. R. (2001) *Chem. Rev.* **101,** 269–295.
26. Marshall, A. G., Hendrickson, C. L. & Jackson, G. S. (1998) *Mass Spectrom. Rev.* **17,** 1–35.
27. Marshall, A. G., Hendrickson, C. L. & Shi, S. D. H. (2002) *Anal. Chem.* **74,** 253A–259A.
28. McLafferty, F. W. (1994) *Acc. Chem. Res.* **27,** 379–386.
29. Anderson, N. L. & Anderson, N. G. (2002) *Mol. Cell. Proteomics* **1,** 845–867.
30. Shimizu, H., Masuta, K., Asada, H., Sugita, K. & Sairenji, T. (2003) *Clin. Chim. Acta* **334,** 233–239.
31. Norman, J. A., Little, D., Bolgar, M. & Di Donato, G. (1991) *Biochem. Biophys. Res. Commun.* **175,** 22–30.
32. Sudoh, T., Kangawa, K., Minamino, N. & Matsuo, H. (1988) *Nature* **332,** 78–81.